

First-principles calculation of the transition temperature T_c for $\text{HgBa}_2\text{CuO}_{4+\delta}$ high-temperature superconductors via dipolon theory

Dale Downs and R. R. Sharma

Department of Physics, University of Illinois at Chicago, Chicago, Illinois 60607-7059

(Received 22 June 1995)

First numerical evaluations of T_c for oxygenated and argon-reduced single-layered $\text{HgBa}_2\text{CuO}_{4+\delta}$ superconductors have been presented. Our calculations are based on the dipolon theory and are found to provide an explanation for the occurrence of superconductivity in single-layered high- T_c superconductors. Relevant expressions useful for the evaluation of T_c have been given. Since the polarizabilities of the ions are not known exactly for the present systems we have performed calculations making use of Pauling's as well as Tessman, Kahn, and Shockley's polarizabilities in order to estimate the uncertainties in the calculated values of T_c associated with uncertainties in the polarizabilities. The effective charges on the ions required for the evaluation of dipoles and dipolon frequencies have been obtained by means of the bond-valence sums. Without fitting with any parameters, our calculations yield T_c values equal to 80 ± 21 K for the oxygenated and 50 ± 27 K for the argon-reduced $\text{HgBa}_2\text{CuO}_{4+\delta}$ superconductors, in agreement with the corresponding experimental values 95 and 59 K. The uncertainties in the calculated values of T_c arise because of the uncertainties in various physical parameters (including polarizabilities) used and due to errors involved in the calculations. The present results are consistent with the observed electronic Raman-scattering intensities which show anomalously broad peaks extended up to several electron volts in cuprate high- T_c superconductors. Our calculated dipolon density of states predict four optical absorption peaks at about 77 cm^{-1} , 195 cm^{-1} , 1.6 eV, and 2.5 eV.

I. INTRODUCTION

Recently, new cuprate superconductors $\text{HgBa}_2\text{Ca}_{n-1}\text{Cu}_n\text{O}_{2n+2+\delta}$ have been discovered with high transition temperatures $T_c \approx 94$,¹ 127,² 134,³ and 126 K (Ref. 4) for $n=1, 2, 3$, and 4 (corresponding to one, two, three, and four CuO_2 layers), respectively. Because of their high T_c values, these compounds are useful for theoretical and experimental studies and technical applications.

The single-layer system $\text{HgBa}_2\text{CuO}_{4+\delta}$ is of particular interest because of its high T_c value and very simple crystal structure consisting of simple tetragonal unit cells. Wagner *et al.*⁵ have made precision measurements of neutron powder diffraction to investigate the defect structure of $\text{HgBa}_2\text{CuO}_{4+\delta}$. The unit cell (simple tetragonal) of the system $\text{HgBa}_2\text{CuO}_{4+\delta}$ as depicted in Fig. 1 contains a single CuO_2 layer with apical oxygens [denoted by O(2)] above and below the Cu ions, forming O(2) layers above and below the CuO_2 layers. The oxygen ions in the CuO_2 layers are denoted by O(1). The oxygen ions at the interstitial site in the Hg a - b plane are referred to as O(3), whereas the oxygen ions in the Hg plane at a site between Hg(Cu_d) sites as O(4). The symbol Cu_d has been used to designate the small amount (~ 0.07) of substitutional Cu on the Hg site.

Wagner *et al.*⁵ have concluded that the single-layered system $\text{HgBa}_2\text{CuO}_{4+\delta}$ contains two defects in the mercury plane of the structure. One of these is the interstitial oxygen [O(3)] defect in the Hg a - b plane. By changing the concentration of this defect from ~ 0.01 to ~ 0.06 , one can vary the T_c value of the sample from 59 to 95 K. The second defect arises from the substitution of a small amount of copper (Cu_d) on the mercury site along with the additional oxygen [O(4)] in the mercury plane (bonded to the copper substitutional defects)

at a site between Hg(Cu_d) sites. They found that the concentration of this defect remains constant, although the concentration of O(3) changes. Also, by making neutron powder diffraction measurements down to 10 K, they observed that the basic structure of the samples remains the same in going

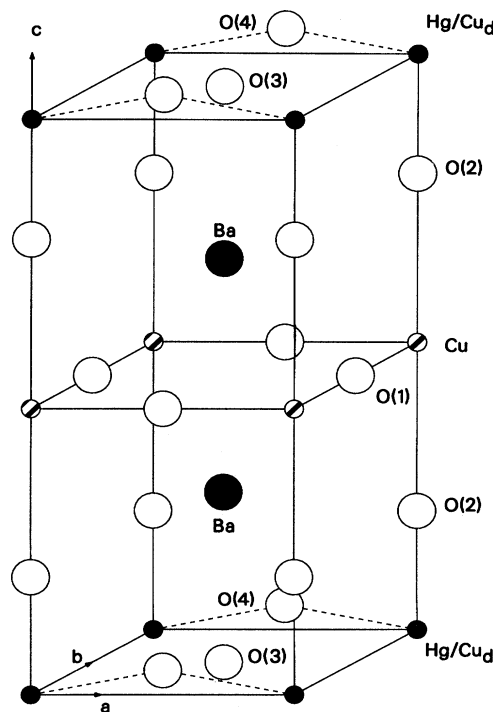


FIG. 1. Depicts a unit cell of $\text{HgBa}_2\text{CuO}_{4+\delta}$.

from normal to the superconducting state.

From a theoretical point of view there are several contending theories⁶ for the high- T_c superconductors (HTS's) based on different pairing mechanisms which involve resonant valence bonds, phonons, antiferromagnetic spin fluctuations, excitons, plasmons, polarons, holons, spinons, anyons, etc. In the framework of the conventional electron-phonon interaction, attempts^{7,8} have also been made by several researchers to understand the superconducting properties in cuprate systems.

The aim of this article is to report our first-principles calculations of T_c , without fitting with any parameters, in oxygenated ($T_c=95$ K) and argon-reduced ($T_c=59$ K) single-layer $\text{HgBa}_2\text{CuO}_{4+\delta}$ superconductors following the microscopic dipolon theory.⁹⁻¹¹ We have selected these systems because, to the knowledge of the authors, no explicit evaluation of T_c for these has yet been reported in the literature and because the dipolon theory has not been previously examined for such single-layer systems.

The dipolon theory is nonphononic in origin and requires dipolon excitations in HTS's. This theory has been found to explain not only the observed T_c and the variation of T_c as a function of the oxygen-stoichiometry parameter δ in $\text{YBa}_2\text{Cu}_3\text{O}_{7-\delta}$ ^{9,10} but also dT_c/dP , the variation of T_c with the hydrostatic pressure P by first-principles calculations without fitting with any parameters, in $\text{YBa}_2\text{Cu}_3\text{O}_{6.93}$ and $\text{YBa}_2\text{Cu}_3\text{O}_{6.60}$.¹¹ Furthermore, the dipolon theory is consistent with the observed isotope effect and the observed optical absorption peaks which are possibly due to the dipolon excitations in the high-temperature superconductors as discussed in Refs. 9 and 10. Specifically, the broad peaks at 2.5 and 0.36 eV in $\text{YBa}_2\text{Cu}_3\text{O}_{7-\delta}$ (Refs. 12, 13) and at 1.0 and 0.17 eV in $\text{La}_{2-x}\text{Ba}_x\text{CuO}_4$ (Refs. 14-19) deduced from the dipolon density of states are in agreement with the optical observations in these systems.

The dipolons are the quantized self-sustained collective excitations^{9,10} of the crystal-field-generated electronic dipoles of the polarizable ions and are mediators (according to the dipolon theory) for the electron-electron (or hole-hole) pairing mechanism (the "dipolon" mechanism) in high- T_c superconductors. The frequencies characteristic of dipolon excitations are shown¹⁰ to be of the order of 1×10^{14} Hz by performing first-principles calculations in several HTS's.

Whereas in the BCS theory the electron-phonon interaction plays part, it is the electron-dipolon interaction which produces an attractive interaction in the dipolon theory. The crystal-field-generated induced dipoles interact cooperatively, giving rise to the dipolon excitations which are quantized and subject to Bose statistics.

In the following section we present the relevant theory applicable to the oxygenated and reduced $\text{HgBa}_2\text{CuO}_{4+\delta}$ single-layer systems. The details of the calculations of the required crystal fields, the induced dipole moments, the dipolon frequencies, and the T_c values making use of the Pauling's^{20,21} as well as the Tessman-Kahn-Shockley (TKS) (Refs. 21, 22) polarizabilities (to obtain uncertainties in calculated T_c values due to uncertainties in the polarizabilities as the exact values of these are not yet known) are given in Sec. III. We discuss our results in Sec. IV where we also present our dipolon density of states for the present systems and predict the optical bands which are possible to be ob-

served. Section V deals with the conclusion.

II. THEORY

The dipolon-mediated pairing interaction is described by⁹

$$V_{ee} = \sum_{\vec{k}\sigma, \vec{k}'\sigma', \vec{q}\lambda} V_{kk'}^{\vec{\sigma}\sigma'} C_{k'\sigma'}^\dagger C_{k\sigma}^\dagger C_{k\sigma} C_{k'\sigma'}, \quad (1)$$

where the pairing potential $V_{kk'}^{\vec{\sigma}\sigma'}$ is given by

$$V_{kk'}^{\vec{\sigma}\sigma'} = \sum_{\lambda} \frac{|h_{kk'\lambda}^{\vec{\sigma}\sigma'}|^2 \hbar \omega_{\vec{q}\lambda}}{[(\epsilon_{\vec{k}} - \epsilon_{\vec{k}'})^2 - (\hbar \omega_{\vec{q}\lambda})^2]}, \quad (2)$$

with

$$h_{kk'\lambda}^{\vec{\sigma}\sigma'} = \sqrt{\frac{\hbar}{16m_e N \omega_{\vec{q}\lambda}}} \sum_{i=1}^{N_d} \frac{4\pi e}{\Omega_0} N' [\vec{p}_0(\vec{\tau}_i) \cdot \hat{q}] \times (\hat{e}_{\vec{q}\lambda} \cdot \hat{q}) \delta_{\vec{k}' - \vec{k}, \vec{q}}. \quad (3)$$

The above equations involve dipolons with wave vector \vec{q} , frequency $\omega_{\vec{q}\lambda}$, polarization mode λ , polarization unit vector $\hat{e}_{\vec{q}\lambda}$, and electrons of mass m_e with wave vectors \vec{k} (or \vec{k}') and spins σ (or σ'). $C_{k'\sigma'}^\dagger$ and $C_{k\sigma}$ are the creation and annihilation operators of the electrons. N is the total number of oscillating dipoles in the crystal of volume Ω_0 containing N' number of unit cells. N_d = number of oscillating dipoles of moment $\vec{p}_0(\vec{\tau}_i)$ present in a unit cell where $\vec{\tau}_i$ describes the position of the dipoles in a cell.

The pairing interaction $V_{kk'}^{\vec{\sigma}\sigma'}$ is attractive in the range $|\epsilon_{\vec{k}'} - \epsilon_{\vec{k}}| < \hbar \omega_{\vec{q}\lambda}$ where $\epsilon_{\vec{k}}$ (or $\epsilon_{\vec{k}'}$) is the electron energy.

The electron-electron interaction described by Eq. (1) is a complicated one. For its evaluation one needs to know not only the dipolon dispersion relations and density of states, but also the electron energy bands. In addition, one then has to follow the complicated theoretical treatment such as the Green's function formulation to calculate T_c with the possibility of losing the basic physics of the problem. Because of this, we adopt the procedure of Refs. 9 and 11 (used in our previous calculations of T_c and dT_c/dP in $\text{YBa}_2\text{Cu}_3\text{O}_{7-\delta}$) to make the pairing potential as an effective potential V .

In the present situation of a single-layer $\text{HgBa}_2\text{CuO}_{4+\delta}$ compound, as will be clear in the next section, we have O(2) as well as O(1) dipolar oscillations contributing to T_c . There are two characteristic frequencies $\omega_d^{(1)}$ and $\omega_d^{(2)}$ corresponding to the dipolar oscillations of O(1) and O(2), respectively. Thus Eq. (2) may be written as

$$V_{kk'}^{\vec{\sigma}\sigma'} = V_{kk'}^{(1)} + V_{kk'}^{(2)}, \quad (4)$$

where ($j=1,2$),

$$V_{kk'}^{(j)} = -V^{(j)} = \begin{cases} -\frac{\pi^2 e^2 \hbar^2 \sum_{i=1}^{N_d^{(j)}} [P_0^{(j)}(\vec{\tau}_i)]^2}{3N' V_c^2 m_e (\hbar \omega_d^{(j)})^2} & \text{for } |\epsilon_{\vec{k}}|, |\epsilon_{\vec{k}'}| < \omega_d^{(j)}, \\ 0 & \text{otherwise,} \end{cases} \quad (5)$$

with $N_d^{(1)}$ and $N_d^{(2)}$ as the number of O(1) and O(2) dipoles of strength $p_0^{(1)}(\vec{\tau}_i)$ and $p_0^{(2)}(\vec{\tau}_i)$, respectively; V_c is the unit cell volume.

Next we make use of the equation for the gap parameter $\Delta(\epsilon)$ at energy ϵ ,

$$\Delta(\epsilon) = -N(\epsilon_F) \int_{-\omega_d}^{\omega_d} d\epsilon' \frac{V_{kk'} \Delta(\epsilon')}{2[\epsilon'^2 + \Delta^2(\epsilon')]^{1/2}} \times \tanh \left(\frac{[\epsilon'^2 + \Delta^2(\epsilon')]^{1/2}}{2k_B T} \right), \quad (6)$$

where k_B is the Boltzmann constant, T is the absolute temperature, and $N(\epsilon_F)$ is the electron density of states at the Fermi energy ϵ_F . In the above equation ω_d in the integration limits are taken as $\omega_d^{(1)}$ or $\omega_d^{(2)}$ according to $V_{kk'}$, as $V^{(1)}$ or $V^{(2)}$.

Then, for the electron-electron pairing potential given by Eq. (4) and for $\omega_d^{(1)} \leq \omega_d^{(2)}$, one deduces the equation useful for obtaining T_c :

$$1 = N(\epsilon_F) V^{(1)} \Phi \left(\frac{\hbar \omega_d^{(1)}}{2k_B T_c} \right) + N(\epsilon_F) V^{(2)} \Phi \left(\frac{\hbar \omega_d^{(2)}}{2k_B T_c} \right) + N(\epsilon_F)^2 V^{(1)} V^{(2)} \Phi \left(\frac{\hbar \omega_d^{(1)}}{2k_B T_c} \right) \left\{ \Phi \left(\frac{\hbar \omega_d^{(1)}}{2k_B T_c} \right) - \Phi \left(\frac{\hbar \omega_d^{(2)}}{2k_B T_c} \right) \right\}, \quad (7)$$

where

$$\Phi(x) = \int_0^x dy \frac{\tanh y}{y}. \quad (8)$$

Equation (7) may also be used for the opposite case $\omega_d^{(1)} \geq \omega_d^{(2)}$ by interchanging the roles of $\omega_d^{(1)}$ and $\omega_d^{(2)}$ and correspondingly the roles of $V^{(1)}$ and $V^{(2)}$.

For evaluation of the $\Phi(x)$ integral for $x < 1$ or ≈ 1 , one may use

$$\Phi(x) = x - \frac{1}{9} x^3 + \frac{2}{75} x^5 - \frac{51}{6615} x^7 + \frac{62}{25 \cdot 515} x^9 - \frac{1382}{1 \cdot 715 \cdot 175} x^{11} + \frac{21 \cdot 844}{79 \cdot 053 \cdot 975} x^{13} - \dots, \quad (9)$$

whereas, for $x \gg 1$,

$$\Phi(x) = \ln(2.28x). \quad (10)$$

Alternately, for any value of x one may use

$$\Phi(x) = \sum_{n=-\infty}^{\infty} \frac{2}{|2n+1|\pi} \arctan \left(\frac{2x}{|2n+1|\pi} \right). \quad (11)$$

For a single cutoff frequency ω_d , Eq. (7) yields

$$k_B T_c = 1.14 \hbar \omega_d \exp \left(- \frac{3N' V_c^2 m_e (\hbar \omega_d)^2}{\pi^2 e^2 \hbar^2 \sum_{i=1}^{N_d} [p_0(\vec{\tau}_i)]^2 N(\epsilon_F)} \right), \quad (12)$$

retrieving the corresponding equation given in Ref. 9.

Because of its complicated structure, Eq. (7) is not amenable to analytical solution for T_c . Thus one has to resort to some numerical technique or to some approximate method.

For the present systems under consideration for which $\omega_d^{(1)}$ is much smaller than $\omega_d^{(2)}$ and for which $\hbar \omega_d^{(1)}/2k_B T_c < 1$ or ≈ 1 , it is possible to obtain a simple expression for T_c provided that one takes the approximation of neglecting the direct coupling of $V^{(2)}$ and $V^{(1)}$ represented by the last term on the right-hand side of Eq. (7). Then one gets, from Eq. (7),

$$k_B T_c = 1.14 \hbar \omega_d^{(2)} \exp \left(- \frac{1}{N(\epsilon_F) V^{(2)}} + \frac{V^{(1)} \hbar \omega_d^{(1)}}{V^{(2)} 2k_B T_c} \right). \quad (13)$$

The above equation is still a complicated one to be solved analytically for T_c because it contains T_c not only on the left-hand side, but also in the exponent on the right-hand side. For the present systems, the $\omega_d^{(2)}$ contribution to T_c is dominant and therefore one may write

$$T_c = T_c^{(2)} \exp \left(\frac{V^{(1)} \hbar \omega_d^{(1)}}{V^{(2)} 2k_B T_c^{(2)}} \right), \quad (14)$$

where $T_c^{(2)}$ is the T_c value as if arising only from the frequency $\omega_d^{(2)}$ and is given by

$$k_B T_c^{(2)} = 1.14 \hbar \omega_d^{(2)} \exp \left(- \frac{1}{N(\epsilon_F) V^{(2)}} \right). \quad (15)$$

Equation (14) is valid if $\hbar \omega_d^{(1)}/2k_B T_c^{(2)} < 1$ or ≈ 1 . If it happens, in some cases, that $\hbar \omega_d^{(1)}/2k_B T_c^{(2)} > 1$, then, instead of Eq. (14), the appropriate expression to be used is

$$T_c = T_c^{(2)} \exp \left\{ \frac{V^{(1)}}{V^{(2)}} \ln \left(2.28 \times \frac{\hbar \omega_d^{(1)}}{2k_B T_c^{(2)}} \right) \right\}, \quad (16)$$

where $T_c^{(2)}$ is given by Eq. (15).

From the above it is evident that one may estimate T_c readily by first obtaining $T_c^{(2)}$ from Eq. (15) and then using appropriately Eqs. (14) or (16). Furthermore, Eqs. (14)–(16) reveal that the effect of $\omega_d^{(1)}$ is to enhance T_c .

As will be clear in the next sections, Eq. (14) [or Eq. (16)] gives a good estimate of T_c for the present systems. However, it must be remarked that, if one does not neglect the last term on the right-hand side of Eq. (7) which represents the direct coupling of $V^{(2)}$ and $V^{(1)}$, the calculated T_c is slightly reduced. This is because $\omega_d^{(1)}$ is smaller than $\omega_d^{(2)}$ for the present systems and consequently this term produces negative effect on the right-hand side in expression (7). This point will be further clear in Sec. III.

III. CALCULATIONS

A. Oxygenated $\text{HgBa}_2\text{CuO}_{4+\delta}$

In order to evaluate T_c from Eqs. (14)–(16) [or from Eq. (7)], we need the induced dipole moments $p_0^{(j)}$'s and the frequencies $\omega_d^{(j)}$'s for the system concerned. To this end one requires information as to the values of the effective charges of the ions in the system which we have calculated by means of the bond-valence sums.^{23,24} According to this, the effective charge $q_{\text{eff}}(i)$ of atom i is

TABLE I. List of sublattice atoms including defects, Pauling's polarizabilities α_i (in units of \AA^3), effective charge of ions $q_{\text{eff}}(i)$ (in units of e), the sublattice and defect coordinates x_i, y_i, z_i (in units of a, b, c , respectively), sublattice and defect occupancies f_i , the calculated electric field due to monopoles $E_z^m(i)$, and the calculated electronic dipoles $p_z(i)$ (in units of $e \text{\AA}$) at various sites in oxygenated $\text{HgBa}_2\text{CuO}_{4+\delta}$. Lattice constants (Ref. 5) used for the calculations are $a=3.8750 \text{\AA}$, $b=3.8750 \text{\AA}$, and $c=9.5132 \text{\AA}$.

Sublattice atom (i)	α_i	$q_{\text{eff}}(i)$	x_i	y_i	z_i	f_i	$E_z^m(i)$	$p_z(i)$
Hg	5.0	2.195	0.0	0.0	0.0	0.93	0.021	~ 0
Cu_d	0.1	0.803	0.0	0.0	0.0	0.07	0.021	~ 0
Ba	1.55	2.073	0.5	0.5	0.2981	1	0.466	0.281
Ba	1.55	2.056	0.5	0.5	0.7019	1	-0.477	-0.279
Cu	0.1	2.099	0.0	0.0	0.5	1	-0.004	~ 0
O(1)	3.88	-2.216	0.5	0.0	0.5	1	-0.003	0.004
O(1)	3.88	-2.216	0.0	0.5	0.5	1	-0.003	0.004
O(2)	3.88	-1.823	0.0	0.0	0.2078	1	0.551	1.180
O(2)	3.88	-1.823	0.0	0.0	0.7922	1	-0.562	-1.195
O(3)	3.88	-0.940	0.5	0.5	0.0	0.059	0.020	0.012
O(4)	3.88	-2.133	0.5	0.0	0.043	0.09	0.268	0.745

$$q_{\text{eff}}(i) = \sum_j s_{ij}, \quad (17)$$

where s_{ij} represents the bond valence or bond strength between the pair of atoms i and j ,

$$s_{ij} = \exp [(r_0 - r_{ij})/B], \quad (18)$$

with r_{ij} representing the distance between the atoms i and j ; r_0 and B are the empirical constants. Setting $B=0.37 \text{\AA}$, the values of r_0 as determined by Brown and Altermatt²⁴ for Hg, Cu, and Ba pairing with oxygen anions are (in units of \AA) 1.972, 1.679, and 2.285, respectively. To calculate the effective charges $q_{\text{eff}}(i)$ in oxygenated $\text{HgBa}_2\text{CuO}_{4+\delta}$, we have made use of the above B and r_0 values and the crystal structure parameters and the occupancies (listed in Table I for easy reference) of the sites including defects as obtained by Wagner *et al.*⁵ The calculated values of $q_{\text{eff}}(i)$ are listed in Table I.

Knowing the values of $q_{\text{eff}}(i)$ and the crystal structure parameters, we have calculated the induced oxygen dipole moments $p_0^{(j)}$, employing the self-consistent method.⁹⁻¹¹ The dipolon frequencies $\omega_d^{(j)}$ have been obtained by means of the dynamic matrix equation, details of which have been furnished in Ref. 10. The crystal fields required for these calculations have been evaluated by direct lattice summation method by forming neutral groups of ions²⁵ to obtain the convergent sums. The accuracy of these results has been verified by performing calculations using *Ewald's* method. The calculated electric fields and dipole moments at various sites are found to be along the c direction as a consequence of symmetry.

The calculated monopole electric fields and the induced dipole moments at various sites using Pauling's polarizabilities (listed also in Table I) (Refs. 20, 21) are tabulated in Table I. The polarizability of Hg has not been known. We have tentatively assigned its value as 5.0\AA^3 . It turns out that the variation in the value of the Hg polarizability does not affect our results because of its location in the crystallo-

graphic cell as is also clear from Table I, which shows that the calculated $p_z(\text{Hg}) \sim 0$. The calculated crystal fields at O(2) located at (0, 0, 0.7922) due to monopoles and self-consistently calculated dipoles using *Pauling's* polarizabilities have been compiled in Table II in order to gain insight into the relative contributions from various ions.

From Table II it is revealed that at the given site O(2) the crystal electric field due to Hg monopoles is a dominant one, whereas the dominant electric field due to dipoles arises from the other O(2) sites. The net electric field due to all monopoles comes out to be about twice of that due to all the dipoles and is of opposite sign. The total electric field due to all the monopoles and all the dipoles equals $-0.308 e/\text{\AA}^2$. This electric field induces a dipole moment on O(2) of magnitude $p_0^{(2)} = 1.20 e \text{\AA}$, listed also in Table III.

It must be pointed out that the direction of the induced dipole of O(2) at (0, 0, 0.2078) is opposite to that of O(2) at (0, 0, 0.7922). Also, because of the occupancy (0.09) of O(4), the electric field at O(2) located at (0, 0, 0.2078) is about 1% lower in magnitude than that at the site (0, 0, 0.7922). Correspondingly, the induced dipole of O(2) at (0, 0, 0.2078) is about 1% smaller in magnitude than that of O(2) at (0, 0, 0.7922). It turns out that incorporation of this slight difference in the magnitudes of the induced dipoles does not alter the value of T_c significantly in the present calculations.

The self-consistent calculation of the electric field at O(1) located at (0, 0.5, 0.5) site is $0.0010 e/\text{\AA}^2$, which is smaller than that at O(2) sites because of large cancellations. The electric field at O(1) located at (0.5, 0, 0.5) is about 2% less than that at O(1) located at (0, 0.5, 0.5) because of the slight occupancy of O(4) sites. Again, this difference does not change the value of T_c significantly. The induced dipole at the O(1) site due to the calculated electric field is $p_0^{(1)} = 0.0039 e \text{\AA}$, listed also in Table III.

Next, we adopt the method of Ref. 10 and make use of the calculated values of the dipoles $p_0^{(j)}$'s to obtain the dipolon frequencies. The calculated maximum dipolon frequencies

TABLE II. Tabulation of the self-consistently calculated electric fields along the c axis, E_z , at an O(2) located at a (0.0,0.0,0.7922) site in oxygenated $\text{HgBa}_2\text{CuO}_{4+\delta}$ as well as at O(2) located at a (0.0,0.0,0.7939) site in reduced $\text{HgBa}_2\text{CuO}_{4+\delta}$ due to the monopoles and the dipoles, using Pauling's polarizabilities, of all the ions in the system; the coordinates of the ions shown in the first column correspond to the oxygenated $\text{HgBa}_2\text{CuO}_{4+\delta}$ and are just to identify the location of the ions in the unit cell. The net result shows the contributions due to all the monopoles and all the dipoles separately. The total result is the sum of the contributions due to all the monopoles and the dipoles in the system.

Due to	Oxygenated $\text{HgBa}_2\text{CuO}_{4+\delta}$		Reduced $\text{HgBa}_2\text{CuO}_{4+\delta}$	
	E_z (monopoles) ($e/\text{\AA}^2$)	E_z (dipoles) ($e/\text{\AA}^2$)	E_z (monopoles) ($e/\text{\AA}^2$)	E_z (dipoles) ($e/\text{\AA}^2$)
Hg	-0.686	~ 0	-0.693	~ 0
Cu_d	-0.019	~ 0	-0.025	~ 0
Ba at (0.5,0.5,0.2981)	0.010	0.024	0.013	0.026
Ba at (0.5,0.5,0.7019)	0.299	0.034	0.306	0.034
Cu	0.410	~ 0	0.395	~ 0
O(1) at (0.5,0.0,0.5)	-0.380	~ 0	-0.379	~ 0
O(1) at (0.0,0.5,0.5)	-0.380	~ 0	-0.379	~ 0
O(2) at (0.0,0.0,0.2078)	0.134	0.111	0.135	0.114
O(2) at (0.0,0.0,0.7922)	0	0.080	0	0.083
O(3)	0.011	~ 0	0.001	~ 0
O(4)	0.039	0.005	0.043	0.005
Net	-0.562	0.254	-0.583	0.262
Total		-0.308		-0.320

corresponding to the longitudinal symmetric modes required for the T_c calculations are $\omega_d^{(2)}=6.3\times 10^{14}$ Hz for the dipolar oscillations of O(2)'s and $\omega_d^{(1)}=0.029\times 10^{14}$ Hz for the dipolar oscillations of O(1)'s as also listed in Table III.

The calculated values $p_0^{(2)}=1.20e \text{\AA}$, $p_0^{(1)}=0.0039e \text{\AA}$, $\omega_d^{(2)}=6.3\times 10^{14}$ Hz, $\omega_d^{(1)}=0.029\times 10^{14}$ Hz, and the available calculated value²⁶ of the electron density of states at the Fermi level, $N(\epsilon_F)=1.46$ states/eV cell, enable us to obtain T_c from Eqs. (14) and (15). From Eq. (15) we get $T_c^{(2)}=61$ K and then, from Eq. (14), $T_c=94$ K, which is amazingly very close to the experimental value 95 K.²⁷ This is very gratifying since no fitting parameters are involved in the present calculations. If one chooses to use the rounded off value of $N(\epsilon_F)$, namely, 1.5 states/eV cell, the calculated value of T_c increases slightly. In this case $T_c^{(2)}=72$ K and, correspondingly, $T_c=101$ K.

Though it appears that, since the dipole of O(1) is much smaller than that of O(2), one could completely neglect

TABLE III. Using Pauling's polarizabilities the calculated oxygen O(2) and O(1) dipoles ($p_0^{(2)}$, $p_0^{(1)}$), the corresponding dipolon frequencies ($\omega_d^{(2)}$, $\omega_d^{(1)}$), and the calculated and experimental values of T_c .

Quantities	Oxygenated $\text{HgBa}_2\text{CuO}_{4+\delta}$	Reduced $\text{HgBa}_2\text{CuO}_{4+\delta}$
$p_0^{(2)}$ ($e \text{\AA}$)	1.20	1.24
$\omega_d^{(2)}$ (10^{14} Hz)	6.3	6.6
$p_0^{(1)}$ ($e \text{\AA}$)	3.9×10^{-3}	4.1×10^{-3}
$\omega_d^{(1)}$ (10^{14} Hz)	0.029	0.031
T_c (K) (Calc.)	80 ± 21	50 ± 27
T_c (K) (Expt.)	95	59

the contribution of the O(1) dipolons. However, our calculations [for $N(\epsilon_F)=1.46$ states/eV cell] reveal that $N(\epsilon_F)V^{(1)}=0.0747$, which is almost half of the calculated value of $N(\epsilon_F)V^{(2)}=0.158$, and thus the contribution of O(1) should not *a priori* be neglected.

Next one inquires what the value of T_c is if one solves Eq. (7) without neglecting the last term which couples $V^{(2)}$ and $V^{(1)}$. We have used an iteration procedure to obtain T_c from Eq. (7), making use of expressions (8)–(11) appropriately. We get $T_c=80$ K, which is somewhat smaller than the T_c obtained by neglecting the last term in Eq. (7).

Clearly, in the above calculations we have made use of the Pauling's polarizabilities.^{20,21} In order to deduce the uncertainty in T_c due to uncertainties in the polarizabilities, we have also performed calculations adopting the TKS polarizabilities of the ions. In this case, because the TKS polarizabilities are smaller than the Pauling's polarizabilities, the calculated dipole moments and, correspondingly, the dipolon frequencies are smaller than those obtained by using the Pauling's polarizabilities. For TKS polarizabilities we obtain $p_0^{(2)}=0.97e \text{\AA}$, $p_0^{(1)}=0.001e \text{\AA}$, $\omega_d^{(2)}=5.1\times 10^{14}$ Hz, and $\omega_d^{(1)}=0.003\times 10^{14}$ Hz. These values using $N(\epsilon_F)=1.5$ states/eV cell yield, from Eq. (15), $T_c^{(2)}=58$ K and, then from Eq. (14), $T_c=85$ K, which is slightly smaller than the T_c value obtained by using Pauling's polarizabilities. On the other hand, Eq. (7), by employing iteration procedure, yields $T_c=60$ K. Thus the TKS polarizabilities tend to give smaller T_c values than those obtained by using Pauling's polarizabilities as expected because the TKS polarizabilities are smaller than the Pauling's polarizabilities.

Considering all of the above results for the oxygenated $\text{HgBa}_2\text{CuO}_{4+\delta}$ (using Pauling's and TKS polarizabilities),

TABLE IV. List of sublattice atoms including defects, Pauling's polarizabilities α_i (in units of \AA^3), effective charge of ions $q_{\text{eff}}(i)$ (in units of e), the sublattice and defect coordinates x_i, y_i, z_i (in units of a, b, c , respectively), sublattice and defect occupancies f_i , the calculated electric field due to monopoles $E_z^m(i)$, and the calculated electronic dipoles $p_z(i)$ (in units of $e \text{\AA}$) at various sites in reduced $\text{HgBa}_2\text{CuO}_{4+\delta}$. Lattice constants (Ref. 5) used for the calculations are $a=3.8888 \text{\AA}$, $b=3.8888 \text{\AA}$, and $c=9.5398 \text{\AA}$.

Sublattice atom (i)	α_i	$q_{\text{eff}}(i)$	x_i	y_i	z_i	f_i	$E_z^m(i)$	$p_z(i)$
Hg	5.0	2.250	0.0	0.0	0.0	0.91	0.019	~ 0
Cu_d	0.1	0.823	0.0	0.0	0.0	0.09	0.019	~ 0
Ba	1.55	2.053	0.5	0.5	0.3016	1	0.485	0.306
Ba	1.55	2.039	0.5	0.5	0.6984	1	-0.496	-0.304
Cu	0.1	2.056	0.0	0.0	0.5	1	-0.004	~ 0
O(1)	3.88	-2.247	0.5	0.0	0.5	1	-0.003	0.004
O(1)	3.88	-2.247	0.0	0.5	0.5	1	-0.003	0.004
O(2)	3.88	-1.780	0.0	0.0	0.2061	1	0.573	1.234
O(2)	3.88	-1.780	0.0	0.0	0.7939	1	-0.583	-1.243
O(3)	3.88	-0.873	0.5	0.5	0.0	0.008	0.019	0.006
O(4)	3.88	-2.091	0.5	0.0	0.036	0.10	0.235	0.657

the calculated values may be expressed as $T_c=80\pm 21$ K (shown also in Table III), compared to the observed $T_c=95$ K (Ref. 27) in this system.

B. Reduced $\text{HgBa}_2\text{CuO}_{4+\delta}$

As the crystal structure parameters and the occupancies are different, we need to calculate $q_{\text{eff}}(i)$ for the reduced $\text{HgBa}_2\text{CuO}_{4+\delta}$ proceeding as above in the case of oxygenated $\text{HgBa}_2\text{CuO}_{4+\delta}$. Making use of the B and r_0 values as given above, the calculated $q_{\text{eff}}(i)$ values obtained by means of bond-valence sums are given in Table IV along with the crystal structure parameters and the occupancies of various sites.⁵

We now use the calculated values of $q_{\text{eff}}(i)$, the crystal structure parameters, and the occupancies of the sites to calculate by direct lattice summation method by forming neutral groups of ions²⁵ to obtain the crystal fields due to monopoles and dipoles employing the self-consistent method.⁹⁻¹¹

The calculated electric monopole fields and the induced dipole moments at various sites using Pauling's polarizabilities (listed also in Table IV) (Refs. 20, 21) are tabulated in Table IV. Here also we have tentatively assigned the Hg polarizability as 5.0\AA^3 . The changes in this value are not found to change our results as it is also clear from Table IV that the induced dipole moment $p_z(\text{Hg})\approx 0$.

The calculated crystal electric fields at O(2) located at (0, 0, 0.7939) due to monopoles and self-consistently calculated dipoles using Pauling's polarizabilities are listed in Table II so as to compare the similar results for the oxygenated $\text{HgBa}_2\text{CuO}_{4+\delta}$ which are already listed in this table. The perusal of the values of the crystal fields listed in Table II shows that the magnitudes of the monopole as well as the dipole electric fields are slightly increased for the case of the reduced $\text{HgBa}_2\text{CuO}_{4+\delta}$ compared to those for the oxygenated $\text{HgBa}_2\text{CuO}_{4+\delta}$ with the result that the induced dipole moment at the O(2) site is slightly larger in the former case. The

calculated dipole moment for O(2) located at (0, 0, 0.7939) in the reduced $\text{HgBa}_2\text{CuO}_{4+\delta}$ comes out to be $1.24e \text{\AA}$, listed also in Table III.

We again find (see also Table IV) that the induced dipole moment of O(2) at (0, 0, 0.2061) is opposite in direction to that of O(2) at (0, 0, 0.7939). Because of the small occupancy (0.10) of O(4), the total electric field at O(2) located at (0, 0, 0.2061) is less than 1% lower in magnitude than that at (0, 0, 0.7939). Consequently, the induced dipole of O(2) at (0, 0, 0.2061) is less than 1% smaller in magnitude than that of O(2) at (0, 0, 0.7939). We have ignored this slight difference in the magnitudes of the dipoles at these two sites as they do not change T_c significantly in our calculations.

The total calculated electric field at O(1) at (0, 0.5, 0.5) is $0.0011 e/\text{\AA}^2$, which is smaller than that at O(2) sites because of cancellation effects. The induced dipole at the O(1) site turns out to be $p_0^{(1)}=0.0041 e \text{\AA}$, listed in Table III.

The calculated values of the dipoles $p_0^{(j)}$'s give the dipole frequencies, $\omega_d^{(2)}=6.6\times 10^{14}$ Hz and $\omega_d^{(1)}=0.031\times 10^{14}$ Hz, tabulated in Table III.

In order to calculate T_c we need to know also the electron density of states at the Fermi level, $N(\epsilon_F)$. The value of $N(\epsilon_F)$ for the reduced $\text{HgBa}_2\text{CuO}_{4+\delta}$ is not known precisely. However, from the electronic band structure calculations by Novikov and Freeman²⁶ and the known occupancies⁵ of the Cu_d , O(4), and O(3) leading to the information as to the doping of the charges in reduced $\text{HgBa}_2\text{CuO}_{4+\delta}$ it is expected that the value of $N(\epsilon_F)$ should lie between 1.3 and 1.5 states/eV cell.

Corresponding to the occupancies of Cu_d , O(3), and O(4), the number of doped holes is approximately equal to 0.33 per cell, which suggests, from the calculations in Ref. 26, that $N(\epsilon_F)\approx 1.33$ states/eV cell. Employing this value of $N(\epsilon_F)$ and the calculated values of $p_0^{(j)}$'s and $\omega_d^{(j)}$'s, one obtains, from Eq. (15), $T_c^{(2)}=25$ K and then (following the required condition), from Eq. (16), $T_c=65$ K, which is close to the experimental value $T_c=59$ K.

If one uses $N(\epsilon_F) = 1.40$ states/eV cell, Eqs. (15) and (16) yield $T_c^{(2)} = 35$ K and $T_c = 77$ K. On the other hand, by iteration technique Eq. (7) yields $T_c = 45$ K for $N(\epsilon_F) = 1.40$ states/eV cell and $T_c = 56$ K for $N(\epsilon_F) = 1.46$ states/eV cell.

As for the results using the TKS polarizabilities, our calculations give T_c values smaller than those obtained by using Pauling's polarizabilities. Explicitly, one gets, from Eqs. (15) and (16), $T_c = 23, 27,$ and 33 K for $N(\epsilon_F) = 1.33, 1.40,$ and 1.46 states/eV cell, respectively. Combining all of the above results for the reduced $\text{HgBa}_2\text{CuO}_{4+\delta}$, one may express $T_c = 50 \pm 27$ K, listed also in Table III.

IV. DISCUSSION

The results in the previous section show that the estimated values of T_c (Table III), 80 ± 21 K for the oxygenated $\text{HgBa}_2\text{CuO}_{4+\delta}$ and 50 ± 27 K for the reduced $\text{HgBa}_2\text{CuO}_{4+\delta}$ are in agreement with the corresponding experimental values.

Our calculations in Sec. III demonstrate that it is easy to estimate the T_c values from the simplified expressions (14)–(16) without resorting to the complicated process of iteration of Eq. (7). Furthermore, these expressions give reasonably good estimates of T_c compared with the experimental values.

For our calculations we have used the $q_{\text{eff}}(i)$ values for various ions as obtained by bond-valence sums. This method gives only an approximate estimate of the effective charges. It is possible that our calculated values of T_c will modify if one uses more precise values of the charges when they are available. However, we do not expect drastic changes in our present calculated values of T_c due to this.

The polarizabilities of the ions, particularly of oxygen, play an important role in our calculations. The exact values of the polarizabilities of oxygen for the present systems are not currently known. It is because of this that we have made calculations using Pauling's and TKS polarizabilities and presented our results in terms of the uncertainties in T_c which account for the uncertainties in the polarizabilities. If the exact values, when available, of the polarizabilities are used, our calculations are not expected to change drastically. Similar conclusion can be drawn from our previous calculations^{9,11} of T_c and T_c versus δ in $\text{YBa}_2\text{Cu}_3\text{O}_{7-\delta}$ systems and variation of T_c with hydrostatic pressure in $\text{YBa}_2\text{Cu}_3\text{O}_{6.60}$ and $\text{YBa}_2\text{Cu}_3\text{O}_{6.93}$.

The occupancies of various sites as given by Wagner *et al.* along with the crystal structure parameters in the present systems show some uncertainties. These uncertainties reflect uncertainties in the estimated electron density of states at the Fermi energy, $N(\epsilon_F)$, as the occupancies of the sites are used in estimating the number of charges doped in the systems, which, in turn, has been used in estimating the value of the associated $N(\epsilon_F)$. It is because of this that we have calculated T_c values for different appropriate values of $N(\epsilon_F)$ in Sec. III in order to find the relevant uncertainties in the calculated values of T_c .

The saddle-point effect on the electron density of states is also important in our calculations since the electron density of states is high near a saddle point (as it is also evidenced from the calculations in Ref. 26) and because the calculated values of Ref. 26 have been used in our estimation of T_c .

To the knowledge of the authors, no explicit calculations

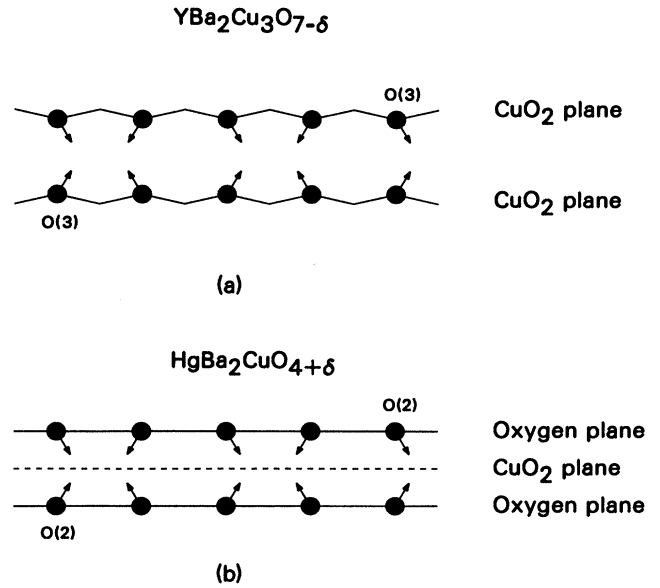


FIG. 2. Displays the cooperative oscillations of the dipoles which contribute dominantly to T_c . (a) For the $\text{YBa}_2\text{Cu}_3\text{O}_{7-\delta}$ system with O(3) dipolar oscillations. (b) For the $\text{HgBa}_2\text{CuO}_{4+\delta}$ system with O(2) dipolar oscillations.

of T_c for the present systems have yet been published in the literature (as also mentioned in Sec. I) for comparison with our results.

As for the comparison with our previous evaluation^{9–11} of T_c and T_c versus δ in $\text{YBa}_2\text{Cu}_3\text{O}_{7-\delta}$ systems and the variation of T_c with hydrostatic pressure in $\text{YBa}_2\text{Cu}_3\text{O}_{6.60}$ and $\text{YBa}_2\text{Cu}_3\text{O}_{6.93}$, we first recall that the dominant contribution to T_c in the $\text{YBa}_2\text{Cu}_3\text{O}_{7-\delta}$ systems arises from the O(3) dipolar vibrations, whereas we find in the present systems that the dominant contribution is from the O(2) dipolar vibrations. More clearly, the perusal of the calculated dispersion relations (not presented here) of the dipolons discloses the fact that in the $\text{YBa}_2\text{Cu}_3\text{O}_{7-\delta}$ systems the O(3)'s from the closely planes vibrate symmetrically so as to contribute to T_c dominantly, whereas in the present systems the (similar) symmetric O(2) vibrations from the nearby O(2) planes give rise to the dominant contribution. This comparison has been displayed pictorially in Fig. 2.

As emphasized in Sec. I, the broad peaks at 2.5 and 0.36 eV in $\text{YBa}_2\text{Cu}_3\text{O}_{7-\delta}$ and at 1.0 and 0.17 eV in $\text{La}_{2-x}\text{Ba}_x\text{CuO}_4$ deduced from the dipolon density of states are in agreement with the optical observations in these systems. This finding has encouraged us to calculate the dipolon density of states also for $\text{HgBa}_2\text{CuO}_{4+\delta}$. Following the procedure of Ref. 10, the calculated dipolon density of states as a function of dipolon frequency for the oxygenated $\text{HgBa}_2\text{CuO}_{4+\delta}$ have been shown in Fig. 3 for dipolons associated with O(1), O(2), O(3), and O(4).

In Fig. 3 the dotted and solid curves correspond to dipolons associated with O(1) and O(3), respectively, whereas the chain-dot and dashed curves correspond to dipolons associated with O(4) and O(2), respectively. To facilitate presentation of our data, the units for the density of states for the

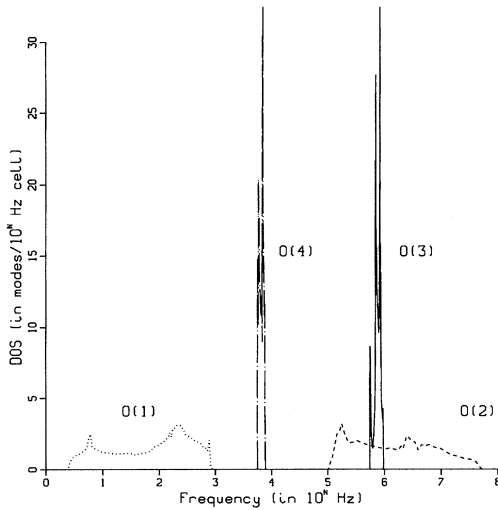


FIG. 3. Plot of dipolon density of states as a function of dipolon frequency associated with O(1) (dotted curve), O(2) (dashed curve), O(3) (solid curve), and O(4) (chain-dot curve) dipolons for oxygenated $\text{HgBa}_2\text{CuO}_{4+\delta}$. To facilitate presentation, the units for the dotted [O(1)] and solid [O(3)] curves are modes/cell $\times 10^{12}$ Hz for the dipolon density of states and 10^{12} Hz for the frequency (corresponding to $N=12$); the units for the chain-dot [O(4)] and the dashed [O(2)] curves are modes/cell $\times 10^{14}$ Hz for the dipolon density of states and 10^{14} Hz for the frequency (corresponding to $N=14$).

dotted [O(1)] and solid [O(3)] curves are taken as modes/cell $\times 10^{12}$ Hz and for the frequency as 10^{12} Hz; the units for the chain-dot [O(4)] and dashed [O(2)] curves are modes/cell $\times 10^{14}$ Hz for the density of states and 10^{14} Hz for the frequency.

From our calculated dipolon density of states, it is possible to predict four optical absorption peaks. First peak corresponds to O(1) dipolons, which lies at nearly 77 cm^{-1} and extends from 13 to 97 cm^{-1} (dotted curve in Fig. 3). The peak which lies at 195 cm^{-1} and extends from 191 to 200 cm^{-1} (solid curve in Fig. 3) is due to O(3) dipolons. The other peaks are due to the O(4) and O(2) dipolons, which lie at nearly 1.59 eV (chain-dot curve in Fig. 3) and 2.5 eV (dashed curve in Fig. 3), respectively. The O(4) peak extends from 1.5 to 1.6 eV , whereas the O(2) peak from 2.1 to 3.9 eV . Hur *et al.*²⁷ have observed a peak close to 195 cm^{-1} in their electronic Raman spectra of $\text{HgBa}_2\text{CuO}_{4+\delta}$, which has not yet been identified. We propose that this peak corresponds to our predicted O(3) dipolons, which is expected to disappear if O(3) defects disappear. Experimentally, Hur *et al.*²⁷ find that this peak disappears when the system becomes pure, which, according to our calculations, is due to reduction (partial or complete, depending on the sample) in the strength of the O(3) dipoles (and correspondingly, the dipolon frequencies) in going from impure to pure systems. Also, the low energy of the experimental peak at 108 cm^{-1} due to plasmons observed in Ref. 27 may be explained by interaction of plasmons with O(1) dipolons.²⁸ This is interesting and important and, hence, warrants further, more careful investi-

gations theoretically as well as experimentally.

Hur *et al.* have not been able to observe our predicted O(4) (1.59 eV) and O(2) (2.5 eV) peaks simply because they have not made observations above 0.09 eV . If the experimental observations are made near 1.6 and 2.5 eV , one expects to observe peaks in the optical spectra corresponding to our predicted 1.59 - and 2.5 -eV peaks. This possibility is also revealed by the fact that the electronic Raman-scattering experiments show unexplained anomalous broad peaks extended up to several electron volts in cuprate high- T_c superconductors.^{12-19,29-34}

Critically, one may argue that the present work is based on pure speculation with dipolon excitations whose existence is rather doubtful. However, this is not so because the existence of the dipolon excitations has already been established theoretically by our first-principles calculations of dipolon excitations and dipolon density of states in several high- T_c superconductors.¹⁰ The experimentally observed broad peaks at 2.5 and 0.36 eV in $\text{YBa}_2\text{Cu}_3\text{O}_{7-\delta}$,^{12,13} the observed broad peaks at 1.0 and 0.17 eV in $\text{La}_{2-x}\text{Ba}_x\text{CuO}_4$,¹⁴⁻¹⁵ and the observed peak in $\text{HgBa}_2\text{CuO}_{4+\delta}$ at about 195 cm^{-1} (as discussed above), which agree with our calculated respective dipolon excitations, provide further proof for the existence of dipolon excitations, particularly when no other (correct) explanation for the appearance of such peaks exists.³⁵ This point is further supported by the fact that the dipolon theory provides possible explanation not only for T_c values in the present systems, but also for the T_c and the variation of T_c as a function of the oxygen-stoichiometry parameter δ in $\text{YBa}_2\text{Cu}_3\text{O}_{7-\delta}$ (Refs. 9, 10) and for the variation of T_c with the hydrostatic pressure, by first-principles without fitting with any parameters, in $\text{YBa}_2\text{Cu}_3\text{O}_{6.93}$ and $\text{YBa}_2\text{Cu}_3\text{O}_{6.60}$.¹¹

V. CONCLUSION

We have made first-principles calculations of T_c for the oxygenated and reduced $\text{HgBa}_2\text{CuO}_{4+\delta}$ in the framework of the dipolon theory. It has been possible to perform these calculations because not only the precise crystal structure parameters are known by powder diffraction method,⁵ but also the calculated values of the electron density of states²⁶ in these systems. We have taken into account the uncertainties in polarizabilities by performing calculations using both the Pauling's and Tessman-Kahn-Schockley polarizabilities as the exact values of the polarizabilities are not yet available. In our calculations we have also estimated the effective charges of the ions by bond-valence sum method^{23,24} in order to estimate the realistic values of the required dipoles and dipolon frequencies. Without fitting with any parameters, the calculated values of T_c are found to be 80 ± 21 and $50 \pm 27 \text{ K}$ for the oxygenated and reduced $\text{HgBa}_2\text{CuO}_{4+\delta}$ systems, respectively, in agreement with the corresponding experimental values 95 and 59 K .⁵ The uncertainties in the calculated values are estimated to be due to uncertainties in various physical parameters (including polarizabilities) and due to calculational errors. We have also been able to predict the possibility of observing four optical absorption peaks at $\sim 77 \text{ cm}^{-1}$, $\sim 195 \text{ cm}^{-1}$, $\sim 1.6 \text{ eV}$, and $\sim 2.5 \text{ eV}$ from our calculated dipolon density of states.

- ¹S. N. Putlin, E. V. Antipov, O. Chmaissem, and M. Marezio, *Nature* **362**, 226 (1993).
- ²S. N. Putlin, E. V. Antipov, and M. Marezio, *Physica C* **212**, 226 (1993).
- ³A. Schilling, M. Cantoni, J. D. Guo, and H. R. Ott, *Nature* **363**, 56 (1993).
- ⁴E. V. Antipov, S. M. Loureiro, C. Caillout, J. J. Capponi, P. Border, J. L. Tholence, S. N. Putlin, and M. Marezio, *Physica C* **215**, 1 (1993).
- ⁵J. L. Wagner, P. G. Radaelli, D. G. Hinks, J. D. Jorgensen, J. F. Mitchell, B. Dabrowski, G. S. Knapp, and M. A. Beno, *Physica C* **210**, 447 (1993).
- ⁶For a review, see P. B. Allen, in *High Temperature Superconductivity*, edited by J. W. Lynn (Springer-Verlag, New York, 1990).
- ⁷*Lattice Effects in high T_c Superconductors*, edited by Y. Bari Yam, T. Egami, J. Mustre-de Leon, and A. R. Bishop (World Scientific, Singapore, 1992).
- ⁸See also J. C. Phillips, *Phys. Rev. Lett.* **72**, 3863 (1994).
- ⁹R. R. Sharma and Heebok Lee, *J. Appl. Phys.* **66**, 3723 (1989); Heebok Lee and R. R. Sharma, *Bull. Am. Phys. Soc.* **33**, 260 (1988).
- ¹⁰Heebok Lee and R. R. Sharma, *Phys. Rev. B* **43**, 7756 (1991).
- ¹¹R. R. Sharma, *Physica C* **224**, 368 (1994).
- ¹²K. Kamaras, C. D. Porter, M. G. Doss, S. L. Herr, D. B. Tenner, D. A. Bonn, J. E. Greedan, A. H. O'Reilly, C. V. Stager, and T. Timusk, *Phys. Rev. Lett.* **59**, 919 (1987).
- ¹³T. Timusk, S. L. Herr, K. Kamaras, C. D. Porter, and D. B. Tenner, *Phys. Rev. B* **38**, 6683 (1988).
- ¹⁴Z. Schlesinger, R. T. Collins, and M. W. Shafer, *Phys. Rev. B* **36**, 5275 (1987).
- ¹⁵S. L. Kerr, K. Kamaras, C. D. Porter, M. G. Doss, D. B. Tenner, D. A. Bonn, J. E. Greedan, C. V. Stager, and T. Timusk, *Phys. Rev. B* **36**, 733 (1987).
- ¹⁶H. P. Geserich, G. Scheiber, and B. Renker, *Solid State Commun.* **63**, 657 (1987).
- ¹⁷S. Etemed, D. E. Espnes, M. K. Kelly, R. Thompson, J. M. Tarascon, and G. W. Hull, *Phys. Rev. B* **37**, 3396 (1988).
- ¹⁸J. Orestein, G. A. Thomas, D. H. Rapkine, C. G. Bethea, B. F. Lavine, B. Batlogg, R. J. Cava, D. W. Johnson, Jr., and E. A. Rietman, *Phys. Rev. B* **36**, 8892 (1987).
- ¹⁹K. Ohbayashi, N. Ogita, M. Udagawa, Y. Aoki, Y. Maeno, and T. Fujita, *Jpn. J. Appl. Phys.* **26**, L240 (1987).
- ²⁰L. Pauling, *Proc. R. Soc. London A* **114**, 181 (1927).
- ²¹C. Kittel, *Introduction to Solid State Physics* (Wiley, New York, 1968), p. 385.
- ²²J. R. Tessman, A. H. Kahn, and Shockley, *Phys. Rev.* **92**, 890 (1953).
- ²³D. Altermatt and I. D. Brown, *Acta Crystallogr. B* **41**, 240 (1985).
- ²⁴I. D. Brown and D. Altermatt, *Acta Crystallogr. B* **41**, 244 (1985).
- ²⁵R. R. Sharma, *Phys. Rev.* **176**, 467 (1968).
- ²⁶D. L. Novikov and A. J. Freeman, *Physica C* **212**, 223 (1993).
- ²⁷N. H. Hur, H. Lee, J. Park, H. Shin, and I. Yang, *Physica C* **218**, 365 (1993).
- ²⁸Heebok Lee and R. R. Sharma, *Phys. Rev. B* **51**, 656 (1995); see also R. R. Sharma, *Bull. Am. Phys. Soc.* **40**, 249 (1995).
- ²⁹D. Reznik, A. Klotz, S. L. Cooper, M. V. Klein, W. C. Lee, and D. M. Ginsberg, *Physica C* **185-189**, 1029 (1991).
- ³⁰S. Sugai, T. Ido, H. Takagi, S. Uchida, M. Sato, and S. Shamoto, *Solid State Commun.* **76**, 365 (1990).
- ³¹T. Staufer, R. Hackl, and P. Muleer, *Solid State Commun.* **75**, 975 (1990).
- ³²M. C. Krantz, H. J. Rosen, J. Y. T. Wei, and D. E. Morris, *Phys. Rev. B* **40**, 2635 (1989).
- ³³F. Slakey, S. L. Cooper, M. V. Klein, J. P. Rice, and D. M. Ginsberg, *Phys. Rev. B* **39**, 2781 (1989).
- ³⁴A. Yamanaka, T. Kimura, F. Minami, K. Inoue, and S. Takekawa, *Jpn. J. Appl. Phys.* **26**, L1902 (1988).
- ³⁵I. Sawada, Y. Ono, T. Matsuura, and Y. Kuroda, *Physica C* **245**, 93 (1995).